CrossMark

SBA-15@methenamine-HPA: a novel, simple, and efficient catalyst for one-pot three-component synthesis of 2-amino-4*H*-chromene derivatives in aqueous medium

Samahe Sadjadi[1] · Majid M. Heravi[2] ·
Vahideh Zadsirjan[2] · Maryam Ebrahimizadeh[2]

Abstract Cl-functionalized SBA-15 was reacted with methenamine and subsequently applied for embedding heteropolyacids. The novel catalyst, SBA-15@methenamine-HPA, was characterized by using scanning electron microscopy (SEM) with energy-dispersive X-ray (EDX) analysis, X-ray diffraction (XRD) analysis, Brunauer–Emmett–Teller (BET) measurements, thermogravimetric analysis (TGA), and Fourier-transform infrared (FTIR) spectroscopy and successfully used for synthesis of a wide range of 2-amino-4*H*-chromene derivatives containing various substituents on the 4*H*-chromene ring through one-pot three-component reaction of aromatic aldehydes, malononitrile, and α-naphthol or β-naphthol in aqueous medium. The catalytic activity of this catalyst was superior to some previously reported conventional catalysts. Moreover, the catalyst was reusable and could be recovered and reused for at least five reaction runs with only slight loss of catalytic activity. The heterogeneous nature of the catalyst, facile workup, excellent yield, and clean, green, and ecofriendly procedure are other advantageous of this protocol.
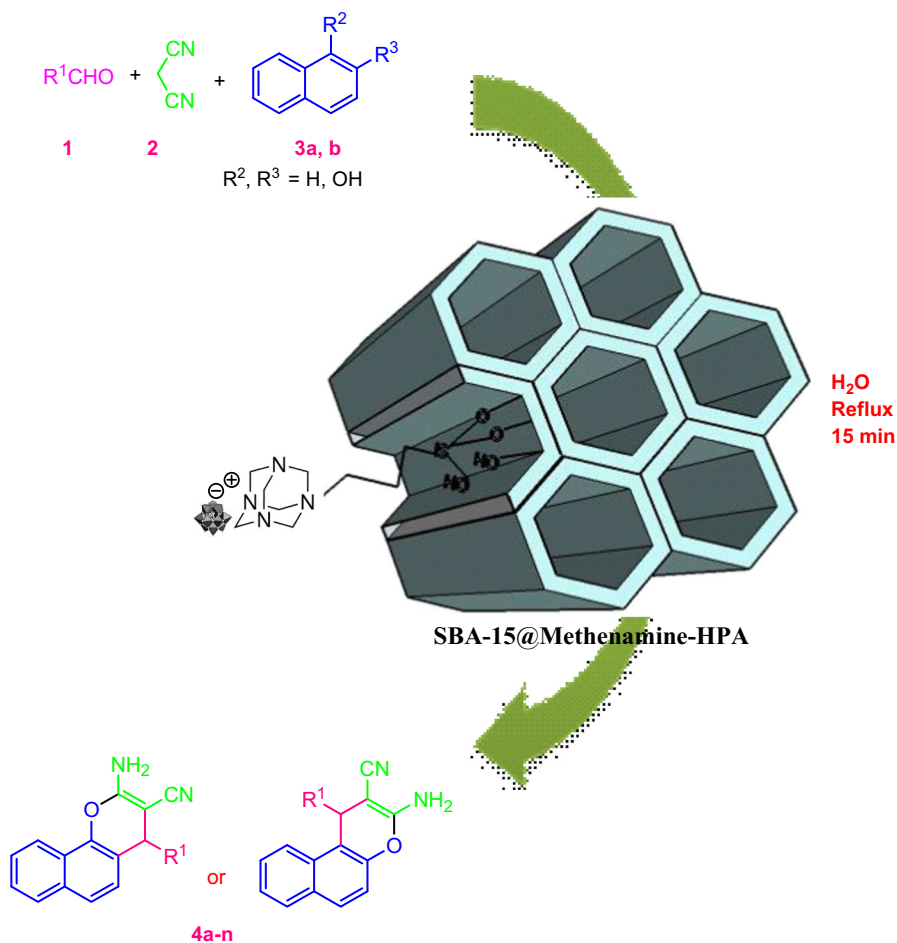
✉ Samahe Sadjadi
samahesadjadi@yahoo.com

✉ Majid M. Heravi
mmh1331@yahoo.com

1 Gas Conversion Department, Faculty of Petrochemicals, Iran Polymer and Petrochemical Institute, PO Box 14975-112, Tehran, Iran

2 Department of Chemistry, School of Science, Alzahra University, PO Box 1993891176, Vanak, Tehran, Iran

Graphical Abstract

SBA-15@Methenamine-HPA

Keywords Heteropolyacid · SBA · Hybrid catalyst · Multicomponent reactions

Introduction

Multicomponent reactions (MCRs) represent a significant approach for development of a range of chemicals including pharmaceuticals, complex organic compounds, and biologically active molecules in a cost- and time-effective manner. MCRs are commonly used for formation of naturally occurring compounds and other biologically active products [1, 2]. Recently, organic syntheses in water in absence of harmful organic solvents have attracted much interest, since water is a safe, cheap, green, and ecofriendly solvent [3, 4].

The 4H-chromene scaffold, a heterocyclic moiety, is present in natural products and motivates pharmaceutically compounds. Fused chromenes are biologically active molecules with a wide range of properties such as antiproliferative [5], mutagenicitical [6], antiviral [7], antimicrobial [8], antitumor [9], sex pheromonal [10], and central nervous system activities [11]. 2-Amino-chromenes are commonly synthesized by refluxing aldehyde, malononitrile, and activated phenols under harmful organic bases such as piperidine in organic solvents including EtOH and MeCN for some hours.

Upon discovery of mesoporous silica materials and their broad range of applications [12, 13] in separation, catalysis [14–18], waste treatment, and sensor design, numerous attempts have been devoted to modification of silica mesoporous materials and development of hybrid systems including them [19]. To date, various hybrid catalysts have been introduced by organic functionalization of ordered mesoporous silica with subsequent incorporation of complexes [20, 21], nanoparticles [22, 23], and heteropolyacids (HPA) [24]. Immobilization of HPA onto mesoporous silica can transform it into a heterogeneous catalyst and improve its catalytic activity through synergistic effects between the silica support and HPA as well as increasing the surface area.

In continuation of our work aimed at developing various novel catalysts for promotion of organic transformations under green and ecofriendly reaction conditions [25–32] and due to the importance of 2-amino-4H-chromene derivatives, we present herein for the first time a novel catalyst based on reaction of Cl-functionalized SBA-15 with methenamine followed by embedding of HPA. The resulting hybrid, SBA-15@methenamine-HPA, serves as a water-tolerant heterogeneous catalyst with excellent activity for synthesis of 2-amino-4H-chromene derivatives (Scheme 1).

Experimental

Materials

The chemicals used for synthesis of the hybrid catalyst included triblock copolymer surfactant (P123), tetraethoxysilane (TEOS), (3-chloropropyl)trimethoxysilane, HCl, methenamine, and phosphomolybdic acid ($H_4[Mo_{12}PO_{40}]$), all provided by Merck. The chemicals applied for studying the catalytic performance were
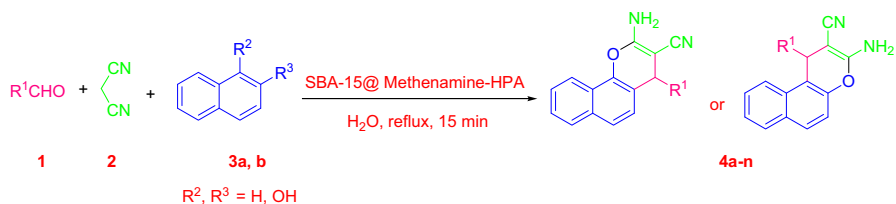
Scheme 1 Synthesis of 2-amino-4H-chromene derivatives

malononitrile, aldehyde derivatives, α-naphthol, and β-naphthol. Starting materials were used as received without any further purification.

Synthesis of SBA-15

Mesoporous silica SBA-15 was synthesized according to previously reported procedure [33]. Typically, deionized water (32 mL) was added to P123 (4.1 g), and the mixture was stirred vigorously. To dissolve P123, a solution of HCl (2 M) was added to the mixture. Upon completion of solvation, TEOS (10 g) was added dropwise. The latter mixture was stirred at 46 °C for 13 h. Subsequently, hydrothermal treatment was performed by transferring the mixture into a Teflon-lined stainless-steel autoclave and keeping it at 103 °C for 24 h. The resulting white solid was filtered, washed repeatedly with deionized water, and calcined at 600 °C for 6 h.

Synthesis of SBA-15-Cl

Cl-functionalized SBA-15 was prepared according to literature [34]. Typically, to suspension of SBA-15 (2 g) in toluene (40 mL), (3-chloropropyl)trimethoxysilane (2 mL) was added. The mixture was subsequently refluxed at 111 °C for 24 h under inert (N_2) atmosphere. Upon completion, the obtained white participate was filtered, washed several times with toluene, and dried at 90 °C overnight.

Preparation of SBA-15@methenamine

SBA-15-Cl (2 g) was added to a flask containing 60 mL dry toluene and methenamine (0.2 g). The resulting mixture was then refluxed at 111 °C for 24 h. Subsequently, the mixture was cooled, filtered, washed with dry toluene, and dried overnight at 100 °C.

Immobilization of HPA onto SBA-15@methenamine: synthesis of SBA-15@methenamine-HPA

Immobilization of HPA onto SBA-15@methenamine was achieved by wet impregnation method. Briefly, solution of HPA (20 wt%) in acetonitrile was added dropwise to suspension of SBA-15@methenamine in acetonitrile. The mixture was stirred at ambient temperature overnight. The obtained precipitate was then filtered, washed with deionized water, and dried at 100 °C overnight. A schematic of the synthetic procedure for the catalyst is depicted in Fig. 1.

Synthesis of 2-amino-4*H*-chromene derivatives

A mixture of a benzaldehyde derivative (1 mmol), malononitrile (1 mmol), α- or β-naphthol (1 mmol), and SBA-15@methenamine-HPA (0.03 g) in water (5 mL) was refluxed at 100 °C for appropriate reaction time. After reaction completion, monitored by thin-layer chromatography (TLC), the mixture was cooled to room
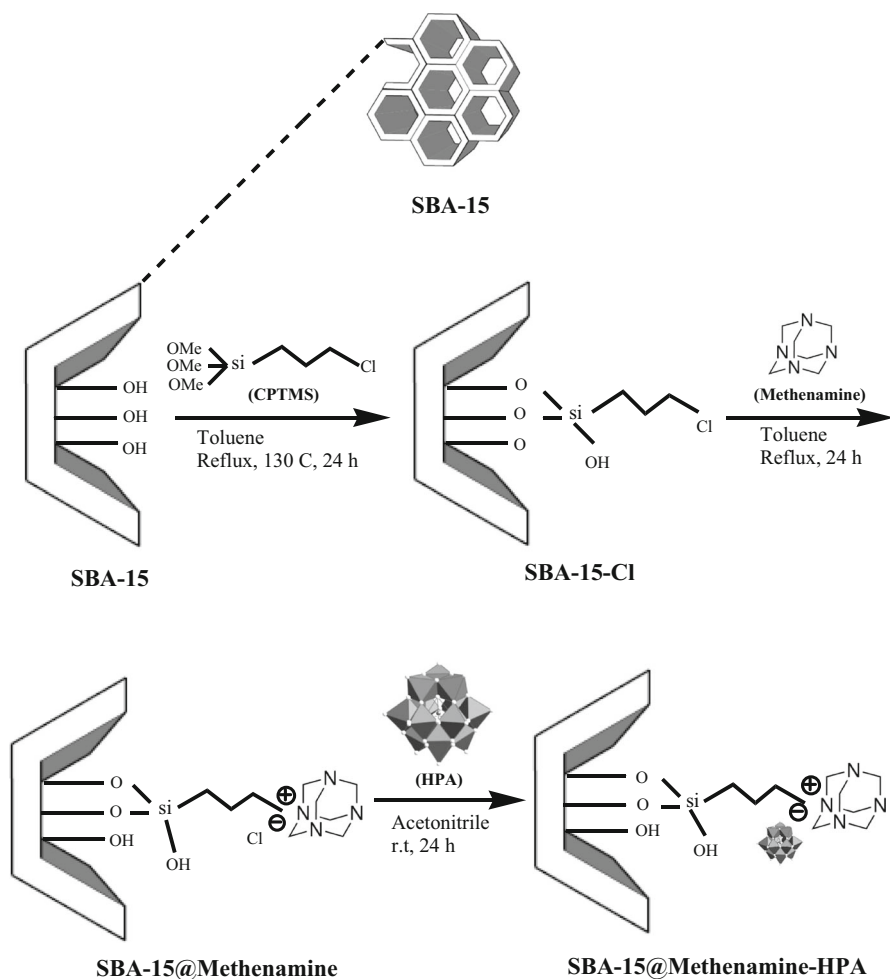
Fig. 1 Schematic of synthetic procedure of catalyst

temperature. The precipitate was collected by filtration and recrystallized from EtOH and H_2O.

Catalyst and product characterization

The obtained catalyst was characterized using various techniques including SEM/EDS, XRD, elemental mapping analysis, and FTIR spectroscopy. SEM/EDS imaging and elemental mapping were carried out on Au-coated samples using a TESCAN instrument at acceleration voltage of 20 kV. The FTIR spectrum was obtained by using a PerkinElmer Spectrum 65 instrument. Room-temperature powder X-ray diffraction patterns were collected using a Siemens D5000 using Cu K_α radiation from a sealed tube. BET analysis was performed via nitrogen

physisorption using a Quantachrome Chem-BET 3000 sorption analyzer (Micromeritics) at 77 K.

Melting points of the synthesized 2-amino-4H-chromene derivatives were measured by using the capillary tube method with an Electrothermal 9200 apparatus and FTIR spectroscopy. All known products were identified by comparison of physical and spectroscopic data with those of previously reported authentic samples.

Physical and spectral data for selected organic compounds

To confirm the formation of the final products, spectral data were obtained for selected products, as presented below, showing results in good agreement with previous reports [26, 35–39], thereby proving the formation of the final products.

2-Amino-3-cyano-4-phenyl-4H-benzo[h]chromene (**4a**) ^{1}H-NMR [400 MHz, dimethyl sulfoxide (DMSO)]: $\delta = 4.90$ (1H, s, H-4), 7.10 (2H, s, NH$_2$), 7.07–7.12 (6H, m, H-5, 2′, 3′, 4′, 5′, 6′), 7.56–7.66 (3H, m, H-6, 8, 9), 7.94 (1H, d, $J = 8.4$ Hz, H-7), 8.23 (1H, d, $J = 8.4$ Hz, H-10) ppm; ^{13}C-NMR (100 MHz, DMSO): $\delta = 41.3$, 54.3, 115.5, 120.8, 121.3, 121.7, 122.4, 123.0, 125.4, 126.3, 127.4, 127.8, 128.4, 130.5, 131.7, 140.4, 142.7, 158.3 ppm. IR (KBr): 3454, 3318, 3020, 2932, 2205, 1656, 1600, 1572, 1450, 1372, 1267, 1100, 1022, 811, 744 cm^{-1}.

2-Amino-3-cyano-4-(4-chlorophenyl)-4H-benzo[h]chromene (**4b**) ^{1}H-NMR (400 MHz, DMSO): $\delta = 4.55$ (1H, s, H-4), 6.70 (2H, s, NH$_2$), 7.1 (1H, d, H-5, $J = 8$ Hz), 7.21–7.33 (4H, m, Ar), 7.40–7.45 (3H, m, Ar), 7.56 (1H, d, H-7, $J = 8$ Hz), 8.15 (1H, d, H-10, $J = 8$ Hz) ppm; ^{13}C-NMR (100 MHz, DMSO): $\delta = 42.6$, 55.6, 119.8, 120.6, 122.1, 122.4, 123.7, 125.4, 125.9, 126.5, 127.6, 128.8, 130.2, 132.8, 133.9, 142.4, 147.6, 160.8 ppm. 132.8, 133.9, 142.4, 147.6, 160.8 ppm. IR (KBr): 3421, 3253, 2208, 1662, 1596, 1436, 1380, 1139, 805 cm^{-1}.

2-Amino-3-cyano-4-(4-nitrophenyl)-4H-benzo[h]chromene (**4c**) ^{1}H-NMR (400 MHz, DMSO): $\delta = 5.12$ (1H, s, H-4), 7.29 (2H, s, NH$_2$), 7.05 (1H, d, $J = 8.4$ Hz, H-5), 7.5–7.7 (3H, m, H-6, 8, 9), 7.52 (d, 2H, H-2′, 6′), 7.90 (1H, d, $J = 8.4$ Hz, H-7), 8.15 (2H, d, H-3′, 5′), 8.27 (1H, d, $J = 8.4$ Hz, H-10) ppm; ^{13}C-NMR (100 MHz, DMSO): $\delta = 43.1$, 54.8, 119.3, 125.7, 121.1, 122.6, 123.6, 124.9, 126.5, 127.2, 128.6, 129.3, 130.6, 133.7, 136.3, 140.9, 146.2, 160.7 ppm. IR (KBr): 3460, 3335, 2196, 1665, 1600, 1575, 1536, 1500, 1346, 1270, 1195, 1100, 805, 770 cm^{-1}.

2-Amino-3-cyano-4-(4-methoxyphenyl)-4H-benzo[h]chromene (**4d**) ^{1}H-NMR (500 MHz, DMSO): $\delta = 3.90$ (3H, s, OCH$_3$), 4.54 (1H, s, H-4), 6.82 (2H, s, NH$_2$), 7.0 (1H, s, H-5, $J = 8$ Hz), 7.10–7.22 (4H, m, Ar), 7.40–7.45 (3H, m, Ar), 7.56 (1H, d, H-7, $J = 8$ Hz), 8.15 (1H, d, H-10, $J = 8$ Hz); ^{13}C-NMR (125 MHz, DMSO): $\delta = 40.8$, 55.1, 56.3, 118.7, 121.9, 122.2, 122.8, 123.5, 124.7, 125.1, 126.9, 127.7, 128.2, 129.4, 131.7, 133.4, 143.5, 148.3, 161.2 ppm. IR (KBr): 3430, 3337, 2200, 1678, 1592, 1436, 1383, 1123, 794 cm^{-1}.

2-Amino-4-(3-nitrophenyl)-4H-benzo[h]chromene-3-carbonitrile (**4e**) ^{1}H-NMR (500 MHz, DMSO): $\delta = 5.24$ (1H, s, H-4), 7.17 (2H, s, NH$_2$), 7.22 (1H, d,

$J = 8.4$ Hz, H-5), 7.29–7.37 (3H, m, H-6, 8, 9), 7.45 (1H, s, H-2′), 7.52–7.63 (3H, m, H-4′, 5′, 6′), 7.82 (1H, d, $J = 8.4$ Hz, H-7), 8.17 (1H, d, $J = 8.4$ Hz, H-10) ppm; ^{13}C-NMR (125 MHz, DMSO): $\delta = 42.7$, 55.7, 120.7, 121.5, 121.8, 122.4, 123.3, 124.2, 125.6, 126.1, 128.2, 128.7, 129.8, 130.3, 132.4, 133.9, 135.7, 141.6, 145.4, 158.3 ppm. IR (KBr): 3404, 3237, 2206, 1674, 1610, 1572, 1521, 1507, 1356, 1261, 1128, 805 cm^{-1}.

2-Amino-4-(4-bromophenyl)-4*H*-benzo[*h*]chromene-3-carbonitrile (**4f**) ^{1}H-NMR (500 MHz, DMSO): $\delta = 4.91$ (1H, s, H-4), 7.06 (1H, d, H-5), 7.19 (2H, m, H-2′, 6′), 7.23 (2H, s, NH$_2$), 7.48 (2H, d, H-3′, 5′), 7.51–7.63 (3H, m, H-6, 8, 9), 7.85 (1H, d, H-7), 8.26 (1H, d, H-10) ppm; ^{13}C-NMR (125 MHz, DMSO): $\delta = 40.2$, 55.8, 117.2, 120.0, 120.2, 120.6, 122.7, 123.9, 125.9, 126.6, 126.7, 127.5, 129.8, 131.5, 132.6, 142.7, 144.9, 160.1 ppm. IR (KBr): 3472, 3329, 2194, 1669, 1601, 1410, 1376, 1103, 780 cm^{-1}.

2-Amino-4-(2,4-dichlorophenyl)-4*H*-benzo[*h*]chromene-3-carbonitrile (**4g**) ^{1}H-NMR (400 MHz, DMSO): $\delta = 5.47$ (1H, s, H-4), 7.30 (2H, s, NH$_2$), 6.98 (1H, d, $J = 8.4$ Hz, H-60), 7.59-7.61 (2H, m, H-3′, 5′), 7.39 (1H, d, H-5), 7.69–7.89 (3H, m, H-6, 8, 9), 8.03 (d, 1H, $J = 8.4$ Hz, H-7), 8.25 (d, 1H, $J = 8.4$ Hz, H 10) ppm; ^{13}C-NMR (100 MHz, DMSO): $\delta = 43.7$, 56.7, 117.5, 119.8120.2, 121.9, 123.2, 124.8, 125.0, 125.3, 127.8, 128.0, 128.6129.7, 131.4, 133.6, 135.2, 141.5, 146.2, 158.7 ppm. IR (KBr): 3454, 3336, 3022, 2182, 1667, 1600, 1572, 1500, 1466, 1378, 1200, 1050, 860, 811, 755 cm^{-1}.

Results and discussion

Catalyst characterization

FTIR analysis was used to confirm incorporation of methenamine and formation of SBA-15@methenamine-HPA (Fig. 2, blue line). The bands observed in the FTIR spectrum clearly demonstrate formation of the SBA-15 framework. The bands at 1068, 790, and 451 cm^{-1} are attributed to stretching of Si–O–Si. The bands at 3386 and 1625 cm^{-1} are attributed to SiO–H and absorbed water, respectively. The band observed at 2913 cm^{-1} is due to –CH$_2$ stretching and proves conjugation of (3-chloropropyl)trimethoxysilane and methenamine. The characteristic band at 1434 cm^{-1} can be assigned to tertiary amine group, which can again be considered as proof for incorporation of methenamine in the catalyst structure. The peaks at 1143, 790, and 931 cm^{-1} can be assigned to symmetric stretching of P–O, Mo–Oe–Mo, and Mo–Ot, respectively [40]. The FTIR spectrum of SBA-15@methenamine-HPA was also compared with that of SBA-15@methenamine (Fig. 2). Obviously, these FTIR spectra are very similar and show the characteristic peaks of SBA-15 and methenamine. However, in the FTIR spectrum of the final catalyst, an additional peak can be observed at 931 cm^{-1}, being representative of HPA.
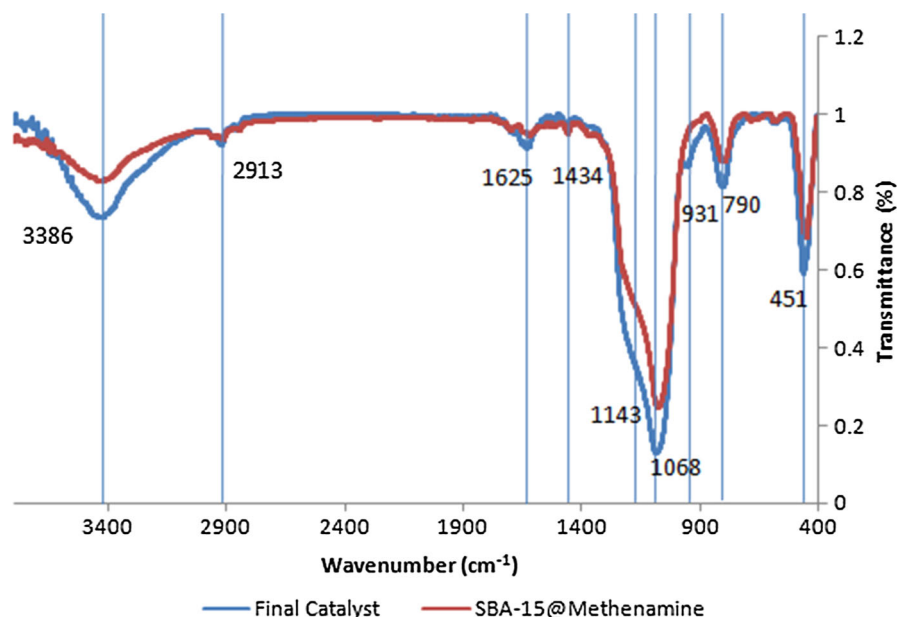
Fig. 2 FTIR spectra of catalyst and SBA-15@methenamine. (Color figure online)

SEM images of SBA-15, SBA-15@methenamine, and SBA-15@methenamine-HPA are depicted in Fig. 2. Obviously, the morphology of the catalyst is different from that of pure SBA-15 (Fig. 3). Pure SBA-15 showed a more compact morphology, while SBA-15@methenamine-HPA showed a more detached morphology. The morphologies of SBA-15@methenamine and SBA-15@methenamine-HPA were similar. However, it is clear that SBA-15@methenamine exhibited a more intertwined morphology. Hence, it can be concluded that introduction of the methenamine motif and HPA can lead to less aggregated morphology. EDX analysis of SBA-15@methenamine revealed Si and O, which can be assigned to the SBA-15 framework, and C and N atoms, which correspond to the organic functionality, methenamine. The presence of P and Mo in EDX analysis of SBA-15@methenamine-HPA demonstrates conjugation of HPA into the catalyst.

The small-angle XRD pattern of the catalyst (Fig. 4) showed three peaks: a sharp peak at 0.9° and two weak peaks at about 1.5° and 1.8°. According to previous reports, these peaks can be assigned to (1 0 0), (1 1 0), and (2 0 0) reflections of the highly ordered periodic arrangement of hexagonal channels [34]. This observation proves that the mesoporous structure of SBA-15 did not collapse upon introduction of methenamine and HPA. According to literature [41], the decrease in intensity of the XRD pattern of the final catalyst may be due to immobilization of methenamine and HPA within pores of SBA-15.

The TGA thermogram of SBA-15@methenamine-HPA is depicted in Fig. 5 (blue line). Obviously, five degradation stages can be observed over the range of 50–600 °C for SBA-15@methenamine-HPA. The first degradation (weight loss at 120 °C) may be due to loss of adsorbed water molecules. Subsequent weight losses
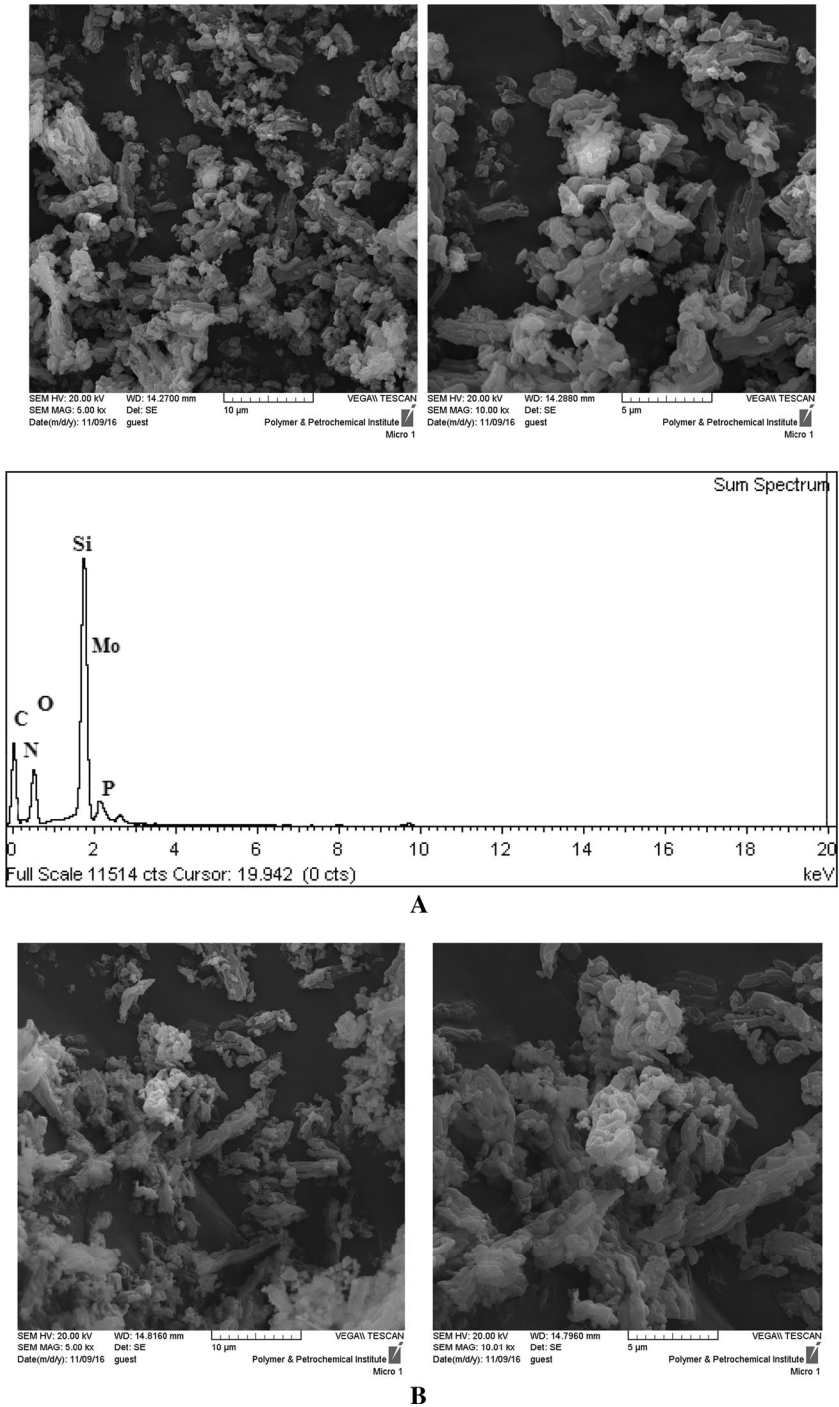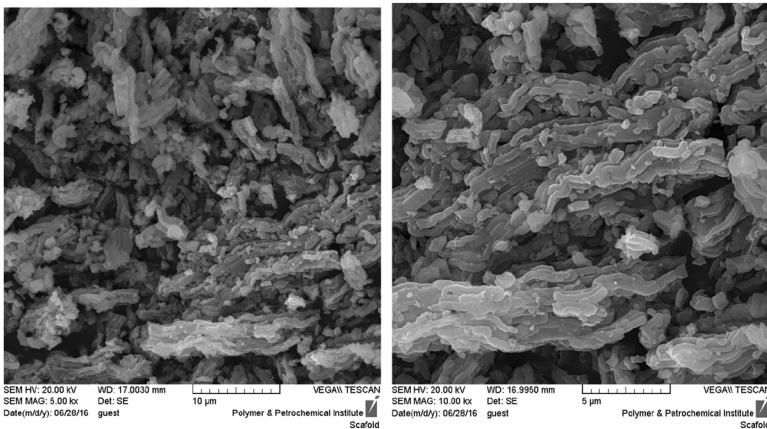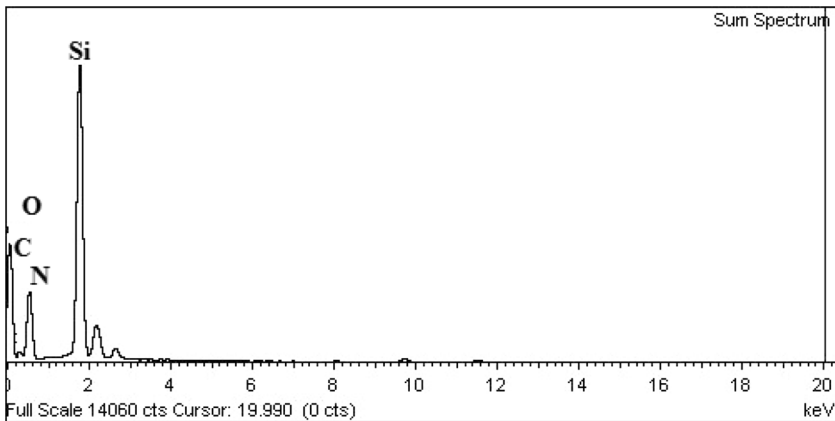
Fig. 3 SEM/EDX images of **a** SBA-15@methenamine-HPA, **b** SBA-15@methenamine, and **c** pure SBA-15

Fig. 3 continued

were observed at about 204, 330, 510, and 600 °C, which can be attributed to thermal decomposition of other components. Using TGA analysis, the content of organic motif was calculated to be about 9 wt%. As a control experiment, the TGA thermogram of SBA-15@methenamine was also obtained (Fig. 5, red line) and compared with that of SBA-15@methenamine-HPA. Four degradation stages can be observed for SBA-15@methenamine, at 140, 220, 370, and 600 °C. As for SBA-15@methenamine-HPA, the first degradation stage is related to loss of water while the remaining stages can be assigned to loss of organic motif.

To estimate the content of HPA in the catalyst, HPA was digested in concentrated hydrochloric and nitric acid solution. Subsequently, the resulting extract was analyzed using inductively coupled plasma (ICP)-atomic emission spectroscopy (AES). Using this method, the loading of HPA was calculated to be about 1 wt%.

The BET surface area of the pure SBA-15 was calculated as 697.7 $m^2 \ g^{-1}$. Incorporation of methenamine and HPA reduced the surface area to 370 $m^2 \ g^{-1}$.
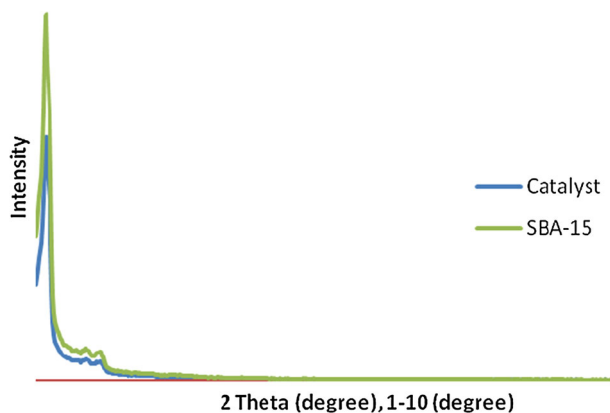
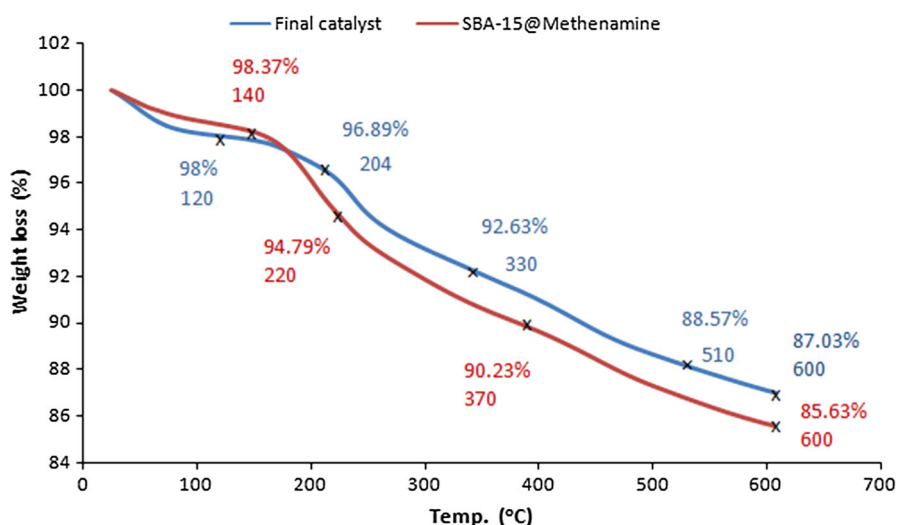**Fig. 4** Small-angle XRD patterns of catalyst and SBA-15. (Color figure online)

Fig. 5 TGA analysis of catalyst and SBA-15@methenamine. (Color figure online)

Catalytic activity

The catalytic activity of the novel hybrid catalyst was tested for formation of 2-amino-4H-chromenes via treatment of aldehyde, malononitrile, and α-naphthol/β-naphthol in aqueous medium under reflux condition. Initially, treatment of benzaldehyde, malononitrile, and α-naphthol in presence of catalytic amount of catalyst was selected as model reaction to determine the optimal conditions (Table 1).

To examine the effects of reaction variables and optimize the reaction condition, a number of experiments with various solvents and quantities of catalyst were carried out (Table 1).

Table 1 Examination of diverse solvents for synthesis of 2-amino-4H-chromenes in presence of SBA-15@methenamine-HPA

Entry	Solvent	Time (min)	Catalyst amount (g)	Yield (%)[a]
1	H_2O	15	0.03	96
2	CH_3CN	120	0.03	70
3	EtOH	60	0.03	80
4	CH_2Cl_2	120	0.03	60
5	Toluene	120	0.03	60
6	DMF	120	0.03	65
7	H_2O	25	0.01	89
8	H_2O	20	0.02	92
9	H_2O	15	0.05	96

[a] Yields refer to isolated products

DMF, dimethylformamide

Table 2 Synthesis of substituted 2-amino-4H-chromenes catalyzed by SBA-15@methenamine-HPA

| Product	R^1	Phenol	Yield (%)[a]	M.p. (°C)	
				Found	Reported
4a	C_6H_5	α-Naphthol	96	209–211	210–211 [37, 38]
4b	$4-ClC_6H_4$	α-Naphthol	93	231–233	232 [37, 38]
4c	$4-NO_2C_6H_4$	α-Naphthol	92	238–240	239.5–241 [37, 38]
4d	$4-MeOC_6H_4$	α-Naphthol	93	189–192	190–191.5 [37, 38]
4e	$3-NOC_6H_4$	α-Naphthol	92	212–215	214.5–216 [37, 38]
4f	$4-BrC_6H_4$	α-Naphthol	89	234–236	234–235 [39]
4g	$4-MeC_6H_4$	α-Naphthol	91	203–306	205–206 [40]
4h	$4-HO-C_6H_4$	α-Naphthol	91	244–247	245 [41]
4i	$4-Me_2N-C_6H_4$	α-Naphthol	90	202–205	203–205 [42]
4j	C_6H_5	β-Naphthol	97	279–281	278–280 [37, 38]
4k	$4-ClC_6H_4$	β-Naphthol	95	206–209	208 [37, 38]
4l	$4-NO_2C_6H_4$	β-Naphthol	93	189–192	188–189 [37]
4m	$4-MeOC_6H_4$	β-Naphthol	94	182–185	182 [37, 38]
4n	$4-BrC_6H_4$	β-Naphthol	91	241–244	241–243 [43]

[a] Yields refer to isolated products

The best yield of the expected product was obtained when using 0.03 g catalyst in H_2O as solvent after 15 min. Armed with this optimal reaction condition, the generality of the reaction was investigated for synthesis of various 2-amino-4H-chromene derivatives. As shown in Table 2, the procedure demonstrated broad substrate scope, and different aldehydes containing electron-donating and electron-withdrawing substituents furnished the desired products in excellent yields. It is important to remark that the nature of the groups on the phenyl ring demonstrated no significant influence when using this route, providing excellent yields in comparatively short reaction times (Table 2) [42–48].

Reaction mechanism

A suggested mechanism for the synthesis of 2-amino-4H-chromenes is shown in Scheme 2 [49]. Initially, the aldehyde **1** reacts with malononitrile **2** to provide α-cyanocinnamonitrile derivative **5**. This stage can be considered as a rapid Knoevenagel addition. The catalyst can accelerate this step of the reaction by activation of the carbonyl group. The second step of the reaction is *ortho* C-alkylation of phenol via reaction with the electrophilic C=C double bond, which can also be promoted by acidic catalyst to afford intermediate **6**. The latter tolerated cyclization through nucleophilic attack of OH substituent on the cyano (CN) scaffold to provide intermediate **7**. Lastly, the desired products **4** were produced through addition and removal of H_2O (7 to 8 to 4).

To study the advantages of the novel catalyst, its activity for synthesis of the model compound was compared with those of previously reported catalysts (Table 3) such as Preyssler heteropolyacid [26], 1,4-diazabicyclo[2.2.2]octane (DABCO) entrapped in agar–agar [50], N,N-dimethylamino-functionalized basic ionic liquid [51], cetyltrimethylammonium bromide [52], γ-alumina [42], $CuSO_4$·$5H_2O$ [53], and potassium hydrogen phthalate [54]. Obviously, compared with most formerly demonstrated catalysts, SBA-15@methenamine-HPA catalyzed the reaction in shorter reaction time. In this context, DABCO entrapped in agar–agar led to the desired product in slightly shorter reaction time. However, the amount of catalyst required was high (1 g), and the solvent was ethanol; Furthermore, the product yield was lower than when using SBA-15@methenamine-HPA. γ-Alumina resulted in comparable yield. However, the reaction time was too long (3 h), and the catalyst amount was twofold that of SBA-15@methenamine-HPA. Compared with heteropolyacid, which is a homogeneous catalyst in water, our proposed catalyst is heterogeneous and can be recovered and reused easily. In the case of using
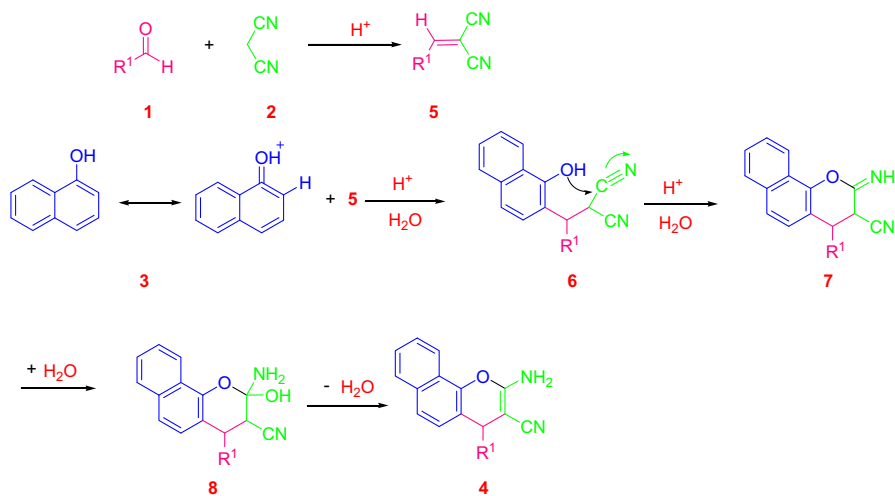
Scheme 2 Possible mechanism for synthesis of compound **4**

Table 3 Comparison of catalytic activity of SBA-15@methenamine-HPA with previously reported catalysts

| Entry	Catalyst	Condition	Time	Solvent	Catalyst amount	Yield (%)	References
1	Preyssler heteropolyacid, $H_{14}[NaP_5W_{30}O_{110}]$	Reflux	3 h	H_2O	0.03 g	91	[26]
2	DABCO entrapped in agar–agar	R.t.	10 min	EtOH	1 g	92	[55]
3	Cetyltrimethylammonium bromide	R.t. (ultrasonic)	2.5 h	H_2O	10 mol%	92	[56]
4	γ-Alumina	Reflux	3 h	H_2O	0.5 g	96	[42]
5	N,N-Dimethylamino-functionalized basic ionic liquid	80 °C	35 min	Solvent free	10 mol%	91	[51]
6	1,8-Diazabicyclo[5.4.0]-undec-7-en-8-ium acetate (DBU[Ac])	80 °C	3 min	Solvent free	10 mol%	93	[57]
7	1,4-Dimethyl-1-(4-sulfobutyl)piperazinium hydrogen sulfate (IL1)	80 °C	3 min	Solvent free	3 mol%	94	[58]
8	1-Butyl-3-methylimidazolium tetrafluoroborate ([bmim]BF₄)	100 °C	90 min	Triethylamine (TEA) in DMF	2 mmol	92	[59]
9	Potassium hydrogen phthalate (KHP)	50 °C	4.5 h	H_2O	25 mol%	90	[54]
10	Nanosized magnesium oxide (MgO)	Reflux	60 min	H_2O	50 mg	86	[60]
11	Potassium phthalimide (POPI)	Ball-milling technique at ambient temperature	10 min	—	5 mol%	97	[61]
12	$CuSO_4 \cdot 5H_2O$	Reflux	90 min	H_2O	5 mol%	98	[53]
13	(4-Dimethylaminopyridine)-functionalized polyacrylonitrile fiber (PANDMAPF)	Reflux	60 min	H_2O	20 mol%	93	[62]
14	Piperidine	Reflux	5 min	H_2O	0.2 mmol	92	[63]
15	Piperidine	Microwave, 80 °C	5 min	EtOH	2 drops	93	[35]
16	SBA-15@methenamine-HPA	Reflux	15 min	H_2O	0.03 g	96	This work
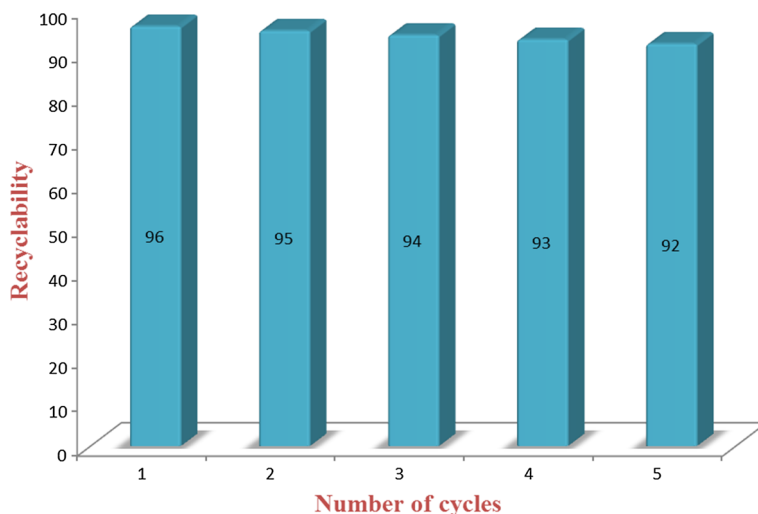
Fig. 6 Recyclability of catalyst for synthesis of 2-amino-4*H*-chromene derivatives

piperidine under microwave or reflux condition, high yields (slightly lower than with SBA-15@methenamine-HPA) were reported. However, that catalyst is homogeneous and toxic. Although using $CuSO_4 \cdot 5H_2O$ as a catalyst under mild reaction temperature led to slightly higher yield, that catalyst also suffers from heterogeneous nature.

Note that the aim herein is to present the catalytic capacity of the novel hybrid SBA-15@methenamine-HPA catalyst, using the synthesis of 2-amino-4*H*-chromene derivatives only as a model organic transformation (Table 3) [26, 35, 42, 51, 53–63].

Catalyst reusability

Finally, we explored the recyclability of the catalyst based on the yield of the desired product of the model reaction when using fresh compared with recycled catalyst (Fig. 6). The results demonstrated that the catalyst could be recovered and reused for at least five reaction runs without significant loss of catalytic property. To explore the leaching of HPA upon recycling and reuse of the catalyst, hot filtration method was applied. The results of ICP analysis showed only negligible leaching of HPA, demonstrating the heterogeneous nature of the catalyst.

Conclusions

We present an extremely significant one-pot multicomponent reaction of aromatic aldehydes, malononitrile, and α-naphthol/β-naphthol in presence of SBA-15@methenamine-HPA under green condition for development of a spectrum of 2-amino-4*H*-chromene derivatives that are frequently employed as pharmacologically and biologically active products. The most significant benefits of this

approach include use of small amount of catalyst, ecofriendly reaction condition, high yield, broad substrate scope, facile and clean workup procedure, and catalyst reusability.

References

1. C. Simon, T. Constantieux, J. Rodriguez, Eur. J. Org. Chem. **2004**, 4957 (2004)
2. M.S. Singh, S. Chowdhury, RSC Adv. **2**, 4547 (2012)
3. P.A. Grieco, Angew. Chem. Int. Ed. **46**, 3798 (2007)
4. C.J. Li, C.J. Li, *Organic Reactions in Aqueous Media* (Wiley, London, 1997)
5. I.H. El Azab, F.M. Abd El Latif, OJSTA **1**, 44 (2012)
6. K. Hiramoto, A. Nasuhara, K. Michikoshi, T. KatoK, K. Kikugawa, Mutat. Res. Genet. Toxicol. Environ. Mutagen. **395**, 47 (1997)
7. P.W. Smith, S.L. Sollis, P.D. Howes, P.C. Cherry, I.D. Starkey, K.N. Cobley, H. Weston, J. Scicinski, A. Merritt, A. Whittington, J. Med. Chem. **41**, 787 (1998)
8. M.M. Khafagy, A.H.F.A. El-Wahab, F.A. Eid, A.M. El-Agrody, Il Farmaco **57**, 715 (2002)
9. S.J. Mohr, M.A. Chirigos, F.S. Fuhrman, J.W. Pryor, Cancer Res. **35**, 3750 (1975)
10. G. Bianchi, A. Tava, Agric. Biol. Chem. **51**, 2001 (1987)
11. F. Eiden, F. Denk, Arch. Pharm. **324**, 353 (1991)
12. B. Karimi, F. Mansouri, M. Khorasani, Curr. Org. Chem. **20**, 349 (2016)
13. G. Mohammadi Ziarani, N. Lashgari, A. Badiei, J. Mol. Catal. **397**, 166 (2015)
14. H. Veisi, A.A. Manesh, N. Eivazi, A.R. Faraji, RSC Adv. **5**, 20098 (2015)
15. H. Veisia, M. Hameliana, S. Hemmati, J. Mol. Catal. A: Chem. **395**, 25 (2014)
16. A. Wach, M. Drozdek, B. Dudek, P. Latka, P. Kustrowski, Microporous Mesoporous Mater. **226**, 433 (2016)
17. X. Song, W. Zhu, K. Li, J. Wang, H. Niu, H. Gao, W. Gao, W. Zhang, J. Yu, M. Jia, Catal. Today **259**, 59 (2016)
18. L. Konga, X. Zhoua, Y. Yaoa, P. Jiana, G. Diaoa, Environ. Technol. **37**, 422 (2016)
19. X. Wang, K.S.K. Lin, J.C.C. Chan, S. Cheng, J. Phys. Chem. B **109**, 1763 (2005)
20. J. Zhang, P. Jiang, Y. Shen, W. Zhang, G. Bian, J. Porous Mater. **23**, 431 (2016)
21. V. Mahdavi, M. Mardani, Res. Chem. Intermed. **41**, 8907 (2015)
22. R.L. Oliveira, W. He, R.J.M. Klein, K. Gebbink, P. de Jong, Catal. Sci. Technol. **5**, 1919 (2015)
23. D. Saikia, Y.-Y. Huang, C.-E. Wu, H.-M. Kao, RSC Adv. **6**, 35167 (2016)
24. X. Sheng, Y. Zhou, Y. Yang, Y. Zhang, Z. Zhang, S. Zhou, X. Fu, S. Zhao, RSC Adv. **4**, 30697 (2014)
25. M.M. Heravi, B. Baghernejad, H.A. Oskooie, J. Chin. Chem. Soc. **55**, 659 (2008)
26. M.M. Heravi, K. Bakhtiari, V. Zadsirjan, F.F. Bamoharram, O.M. Heravi, Bioorg. Med. Chem. Lett. **17**, 4262 (2007)
27. M.M. Heravi, E. Hashemi, Y. Shirazi Beheshtiha, S. Ahmadi, T. Hosseinnejad, J. Mol. Catal. A **394**, 74 (2014)
28. M.M. Heravi, F. Mousavizadeh, N. Ghobadi, M. Tajbakhsh, Tetrahedron Lett. **55**, 1226 (2014)
29. S. Sadjadi, M.M. Heravi, Curr. Org. Chem. **20**, 1404 (2016)
30. M.M. Heravi, M. Saeedi, Y.S. Beheshtiha, H.A. Oskooie, Mol. Divers. **15**, 239 (2011)
31. M.M. Heravi, S. Sadjadi, J. Iran. Chem. Soc. **6**, 1 (2009)
32. M.M. Heravi, S. Sadjadi, N.M. Haj, H.A. Oskooie, F.F. Bamoharram, Catal. Commun. **10**, 1643 (2009)
33. M. Hami Dindar, M.R. Yaftian, M. Hajihasani, S. Rostamnia, J. Taiwan Inst. Chem. Eng. **67**, 325 (2016)
34. H. Li, M. Yang, Q. Pu, Microporous Mesoporous Mater. **148**, 166 (2012)
35. R. Mekheimer, K. Sadek, J. Heterocycl. Chem. **46**, 149 (2009)
36. T. Jin, J. Xiao, S. Wang, T. Li, Ultrason. Sonochem. **11**, 393 (2004)

37. M. Heravi, K. Bakhtiari, V. Zadsirjan, F. Bamoharram, O. Heravi, Bioorg. Med. Chem. Lett. **17**, 4262 (2007)
38. D. Shi, S. Zhang, Q. Zhuang, X. Wang, S. Tu, H. Hu, Chin. J. Chem. **23**, 1419 (2003)
39. M. Naimi-Jamal, S. Mashkouri, A. Sharifi, Mol. Divers. **14**, 473 (2010)
40. A. Aouissi, Z.A. Al-Othman, H. Al-Anezi, Molecules **15**, 3319 (2010)
41. L. Li, J. Shi, Chem. Commun. 996 (2008)
42. R. Maggi, R. Ballini, G. Sartori, R. Sartorio, Tetrahedron Lett. **45**, 2297 (2004)
43. T.S. Jin, J.-C. Xiao, S.-J. Wang, T.-S. Li, Ultrason. Sonochem. **11**, 393 (2004)
44. R.C. Popescu, M.O. Fufa, A.M. Grumezescu, Rom. J. Morphol. Embryol. **56**, 635 (2015)
45. J.M. Khurana, B. Nand, P. Saluja, Tetrahedron **66**, 5637 (2010)
46. B.S. Kumar, N. Srinivasulu, R.H. Udupi, B. Rajitha, Y.T. Reddy, P.N. Reddy, P.S. Kumar, J. Heterocycl. Chem. **43**, 1691 (2006)
47. T.-S. Jin, J.-C. Xiao, S.-J. Wang, T.-S. Li, X.-R. Song, Synlett **2003**, 2001 (2003)
48. N.V. Shitole, K.F. Shelke, S.A. Sadaphal, B.B. Shingate, M.S. Shingare, Green Chem. Lett. Rev. **3**, 83 (2010)
49. J. Bloxham, C.P. Dell, C.W. Smith, Heterocycles **38**, 399 (1994)
50. S. Shinde, G. Rashinkar, R. Salunkhe, J. Mol. Liq. **178**, 122 (2013)
51. L. Chen, X.-J. Huang, Y.-Q. Li, M.-Y. Zhou, W.-J. Zheng, Monatsh. Chem. **140**, 45 (2009)
52. T.-S. Jin, J.-C. Xiao, S.-J. Wang, T.-S. Li, Ultrason. Sonochem. **11**, 393 (2004)
53. F. Behbahani, M. Sadeghi, J. Korean Chem. Soc. **57**, 357 (2013)
54. H. Kiyani, F. Ghorbani, Res. Chem. Intermed. **41**, 7847 (2015)
55. S. Shinde, G. Rashinkar, R. Salunkhe, J. Mol. Liq. **178**, 122 (2013)
56. T.-S. Jin, J.-C. Xiao, S.-J. Wang, T.-S. Li, Ultrason. Sonochem. **11**, 393 (2004)
57. D. Habibi, A. Shamsian, J. Chem. Res. **37**, 253 (2013)
58. D. Habibi, A. Shamsian, D. Nematollahi, Chem. Pap. **69**, 586 (2015)
59. S. Kanakaraju, B. Prasanna, S. Basavoju, G. Chandramouli, J. Mol. Struct. **1017**, 60 (2012)
60. D. Kumar, V. Reddy, B. Mishra, R. Rana, M. Nadagouda, R. Varma, Tetrahedron **63**, 3093 (2007)
61. M.G. Dekamin, M. Eslami, Green Chem. **16**, 4914 (2014)
62. Y. Zhen, H. Lin, S. Wang, M. Tao, RSC Adv. **4**, 26122 (2014)
63. G. Lu, C. Cai, J. Heterocycl. Chem. **48**, 124 (2011)